Adaptive Compensation Loop Control Method for Dynamic Range Wireless Power Transfer in Endoscopic Capsules Applications

Hao Zhang [1,2], Zheng Zhong [2], and Wen Wu [1]

[1] School of Electronic and Optical Engineering
Nanjing University of Science and Technology, Nanjing, 210094, China
18501566409@163.com, wuwen@mail.njust.edu.cn

[2] Department of Electrical and Computer Engineering
National University of Singapore, Singapore, 117583, Singapore
elezhon@nus.edu.sg

Abstract ─ In this paper, an adaptive compensation loop control method is presented for dynamic range wireless power transfer (WPT) based wireless endoscopic capsules (WEC) applications. Rather than a fixed external resistor feedback network utilized in the DC-DC converter with maximum power point control (MPPC) capability, an enhanced nMOSFET based adaptive compensation loop is introduced to extract maximum power transfer from the RF-DC rectifier within overall operational power range of the WEC system. Simulation in ADS and measurement among three rectifiers with an LDO, a fixed external resistor feedback network and an adaptive compensation loop control are performed respectively to achieve a steady 3.3V on a resistive load of 100Ω, which validates that the proposed adaptive compensation loop control method realizes an extended dynamic power range with a lower limit of 21.5dBm to realize a minimum 100mW load DC power delivery for the IPT enabled WEC system.

Index Terms ─ Adaptive compensation loop, dynamic range, enhanced nMOSFET, MPPC, resistor feedback network, WEC, WPT.

I. INTRODUCTION

Wireless endoscopic capsules (WEC) technology has been developing and researching rapidly in recent years since it provides an alternative solution to the traditional endoscopies for the painless diagnosis of cancer or other diseases affecting the gastrointestinal tract [1]. It releases patients from the painful surgical operations thanks to its specific attributes of the convenience and non-invasion compared with a traditional endoscopy, which enables the patients to have more comfortable medical check-ups and allow a doctor to get a comprehensive profile of the patients' physiological conditions.

However, the power capacity limitation of the cell batteries has become a bottleneck in the WEC's wide applications. Typically, an inductive power transfer (IPT) [2] is introduced to get rid of this constraint (see Fig. 1). A receiving coil captures the alternative magnetic field generated by a transmitting coil to convert into the alternative electrical field as a power source. Then this portion of power is delivered into an RF-DC rectifier for the rectification to achieve a direct voltage V_{in}. However V_{in} is usually not stable for the DC voltage supply requirement of some commercial electronics, such as a micro-programmable control unit (MCU) and sensors. Therefore it's needed to regulate V_{in} by a DC-DC converter (see Fig. 1). In the traditional IPT system, a low dropout (LDO) regulator is typically adopted as the DC-DC converter. When V_{in} is slightly more than the rated operational voltage V_o, LDO is an effective and simple choice for the battery-powered applications [3]. Nevertheless, if V_{in} is much more than V_o, LDO will introduce much power loss as its operation mechanism is only to regulate V_{in} without considering the DC-DC conversion efficiency.

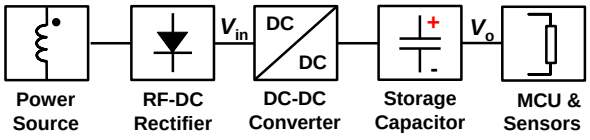

Fig. 1. Block diagram of a IPT receiver.

Therefore, it's essential to adopt a DC-DC bulk with a maximum power point control (MPPC) capability instead of a traditional LDO, which enables a maximum power transfer extraction from a non-ideal DC voltage source when V_{in} is much more than V_o in the IPT system. Nevertheless, some commercial DC-DC converters (e.g., LTC3129-1) can only be controlled with a fixed external

Submitted On: September 30, 2017
Accepted On: April 10, 2018

high resistor feedback network, which maximizes power transfer from a specific and fixed non-ideal DC voltage source [4].

In this paper, rather than a fixed external high resistor feedback network employed in the DC-DC converter, an enhanced nMOSFET Si2342DS based adaptive compensation loop control is proposed to extract the maximum power transfer from the HSMS282P based voltage doubler rectifier over a wide dynamic range of the WEC system. Measurement and fabrication validate that the proposed adaptive compensation loop control enables an extended dynamic power range with a lower limit of 21.5dBm (22.5dBm for the fixed external high resistor network and 25dBm for the LDO SPX3819 in our previous work [8]) to realize a minimum 100mW load DC power delivery, which brings a practicality for the IPT enabled WEC applications.

II. THEORY ANALYSIS

To maximize power extraction from a non-linear DC power source, the DC-DC converter maximum power transfer incident voltage $V_{\text{in(MPPC)}}$ can be controlled by a constant external resistor feedback network consisting of two high resistors R_{high} and R_{low} as:

$$V_{\text{in(MPPC)}} = V_{\text{ref}}\left(\frac{1 + R_{\text{low}}/R_{\text{high}}}{R_{\text{low}}/R_{\text{high}}}\right), \qquad (1)$$

where V_{ref} is the reference voltage of the implemented DC-DC converter (e.g., V_{ref} =1.175V in LTC3129-1).

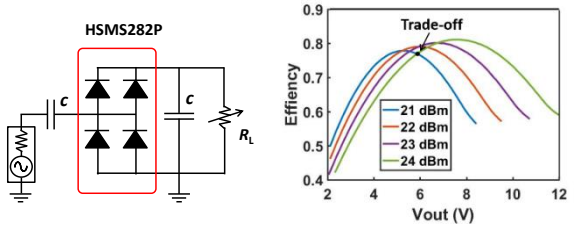

(a) (b)

Fig. 2. (a) HSMS282P based voltage doubler rectifier; (b) power conversion efficiency versus output voltage.

However, the RF-DC rectifier, as a non-ideal power source, can generate different $V_{\text{in(MPPC)}}$ as the incident voltage supply of the LTC3129-1 within various incident powers [5]. Therefore, it addresses an extreme challenge for the fixed voltage $V_{\text{in(MPPC)}}$ in (1) to extract a maximum power transfer within a wide dynamic range IPT enabled WEC system, which requires an adaptive compensation loop to dynamically adjust the ratio of $R_{\text{low}}/R_{\text{high}}$. For the validation, a HSMS282P based voltage doubler rectifier (see Fig. 2 (a)) is designed with harmonic balance (HB) simulation in ADS at 200KHz by sweeping a resistive load R_{L}. Incident power varies from 21dBm to 24dBm, which covers a WEC system's operational power range. Parallel-diode topology of HSMS282P is implemented to reduce the semiconductor resistive loss of R_{s} in its current path when charging and discharging during the procedure of RF-DC rectification [6]. Power conversion efficiency versus output voltage is then calculated in Fig. 2 (b). Thus $V_{\text{in(MPPC)}}$ of HSMS282P based voltage doubler rectifier with the maximum power transfer efficiency is confirmed to be increased with its incident powers [5]. When a trade-off $V_{\text{in(MPPC)}}$=6V is selected with a fixed ratio $R_{\text{low}}/R_{\text{high}}$ around 0.24, a maximum overlap RF-DC conversion efficiency of 74% can only be achieved over power range from 21dBm to 24dBm. Even worse, when the IPT receiver acquires more conversion efficiency, there may be no trade-off $V_{\text{in(MPPC)}}$ for the input voltage supply of the DC-DC converter, which degrades a WEC system performance considerably. Detailed simulation and calculation of a HSMS282P based voltage doubler rectifier (see Fig. 2 (a)) is provided in Table 1 over the WEC operational power range from 21dBm to 24dBm. $V_{\text{in(MPPC)}}$ of the implemented DC-DC converter equals output voltage V_{out} with the maximum power conversion efficiency $E_{ff\text{max}}$ in Fig. 2 (b). Ratio of $R_{\text{low}}/R_{\text{high}}$ can be calculated by reference to the Equation (1). Consequently, $V_{\text{in(MPPC)}}$, $E_{ff\text{max}}$ and $R_{\text{low}}/R_{\text{high}}$ can be determined within different power levels (i.e., Table 1). Noticeably, it's observed an obvious $R_{\text{low}}/R_{\text{high}}$ variation occurs, which seriously degrades the $V_{\text{in(MPPC)}}$ extraction for the LTC3129-1 to maximize power transfer from a non-ideal DC voltage source (i.e., a rectifier in Fig. 2 (a)).

Table 1: Simulation data of the rectifier in Fig. 2 (a)

P_{in} (dBm)	$V_{\text{in(MPPC)}}$ (V)	$E_{ff\text{max}}$ (%)	$R_{\text{low}}/R_{\text{high}}$
21	5.27	79	0.29
22	5.98	79.2	0.25
23	6.74	80.1	0.21
24	7.61	81.1	0.18

So as to get rid of the constraint mentioned, ratio of $R_{\text{low}}/R_{\text{high}}$ in the external high resistor feedback network should be compensated dynamically to achieve $V_{\text{in(MPPC)}}$ within different incident power levels. In order to enable a simple and compact circuit, dynamic adjustment of R_{low} is introduced in this research. Moreover, the voltage drop along R_{low} is constant and equal to the internal V_{ref} of 1.175V [4] under maximum power transfer condition of HSMS282P based voltage doubler based rectifier. Thus, an initial rectifier design with an adaptive loop control is proposed in Fig. 3 with a compensation resistor R_{c}, which functions to dynamically adjust the current (i.e., I_3) in the external high resistor feedback network.

When input power increases, the output current I_1 of RF-DC rectifier rises accordingly along with the input voltage V_{in}. Then it requires a higher $V_{\text{in(MPPC)}}$ for the input supply of the LTC3129-1 in Table 1 to extract the maximum power transfer efficiency. Therefore the compensation resistor R_{c} should be reduced to increase

I_3 until the voltage at MPPC pin equals the internal reference V_{ref}. Then the input voltage $V_{in(MPPC)}$ of the DC-DC converter can be expressed:

$$V_{\text{in(MPPC)}} = V_{\text{ref}} + R_{\text{high}} I_3. \tag{2}$$

In this research, an enhanced nMOSFET based compensation control is introduced to function as R_c in Fig. 3. Typically V_{GS} biased nMOSFETs are applied to achieve a variable resistor in its deeply linear operational region and the drain-to-source channel current I_D before approaching its saturation value can be expressed as:

$$I_{\text{D}} = \mu_{\text{n}} C_{\text{ox}} \frac{W}{L}\left[(V_{\text{GS}} - V_{\text{TH}})V_{\text{DS}} - \frac{1}{2}V_{\text{DS}}^2\right], \tag{3}$$

where W is gate width, L is gate length, μ_n is a foundry concerned constant, C_{ox} is the capacitance in the oxide layer and V_{TH} is the intrinsic threshold voltage.

Therefore V_{GS} controls the value of channel current I_D. When I_D reaches its saturation with $V_{DS} \geq V_{GS}-V_{TH}$, the maximum channel current remains constant as:

$$I_{\text{D,max}} = \frac{1}{2}\mu_{\text{n}} C_{\text{ox}} \frac{W}{L}(V_{\text{GS}} - V_{\text{TH}})^2. \tag{4}$$

Typically, if $V_{DS} << 2(V_{GS}-V_{TH})$, the nMOSFET operates in its deeply linear operational region and the DC-IV characteristic can be simplified as:

$$I_{\text{D}} \approx \mu_{\text{n}} C_{\text{ox}} \frac{W}{L}(V_{\text{GS}} - V_{\text{TH}})V_{\text{DS}}. \tag{5}$$

Thus, the drain-to-source channel can be expressed as a V_{GS} controllable resistor R_{DS}:

$$R_{\text{DS}} = \frac{1}{\mu_{\text{n}} C_{\text{ox}} \frac{W}{L}(V_{\text{GS}} - V_{\text{TH}})}. \tag{6}$$

Then R_{DS} is regarded as a linear function of V_{DS} when V_{GS} remains constant. However, when V_{GS} decreases, R_{DS} increases inversely. Therefore, variable drain-to-source channel resistor R_{DS} can be realized with variation of V_{GS}. However, the value of R_{DS} in its deeply linear operational region of nMOSFET is typically not high enough for the compensation resistor R_c variation requirement in Fig. 3.

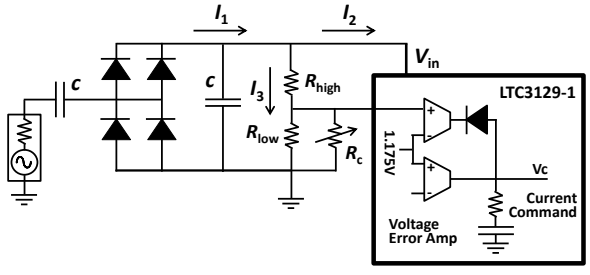

Fig. 3. Proposed circuit with a compensation resistor R_c.

In order to realize an efficient adaptive compensation control loop design, the internal reference voltage V_{ref} of the implemented DC-DC converter is utilized. As shown in Fig. 3, the function of R_c is to dynamically adjust I_3 through the external high resistor feedback network. Rather than the application of R_{DS} in its deeply linear region, V_{GS} biased nMOSFET current source is adopted to enable the current I_3 control with V_{DS} equal the internal voltage reference V_{ref} of the implemented DC-DC bulk under the maximum transfer from the rectifier in Fig. 2 (a). Therefore, V_{GS} biased current source can replace R_c to behave like an equivalent enhanced variable resistance $R_{DS,en}$, which functions to dynamically adjust I_3 within different powers. When $V_{DS} \geq V_{GS}-V_{TH}$, I_D maintains its maximum value $I_{D,max}$ in (4). Hence, the drain-to-source channel can still be controlled by the V_{GS} while V_{DS} maintains constant with V_{ref} of 1.175V. Under this condition, the equivalent enhanced $R_{DS,en}$ functions as the compensation R_c:

$$\begin{aligned} R_{\text{DS,en}} &= \frac{V_{\text{DS}}}{I_{\text{D,max}}} = \frac{2V_{\text{DS}}}{\mu_{\text{n}} C_{\text{ox}} \frac{W}{L}(V_{\text{GS}} - V_{\text{TH}})^2} \\ &= \frac{2V_{\text{DS}}}{(V_{\text{GS}} - V_{\text{TH}})} R_{\text{DS}}. \end{aligned} \tag{7}$$

Therefore, the current I_3 adjusting capability from R_{DS} is enhanced by a coefficient of $2V_{DS}/(V_{GS}-V_{TH})$ when $V_{DS}=V_{ref} \geq V_{GS}-V_{TH}$ under the maximum power extraction from the rectifier in Fig. 2 (a). When an ultra-small V_{GS} is selected, the ultra-high channel equivalent $R_{DS,en}$ in (7) can be realized to satisfy R_c requirements for I_3 current variation in the external high resistor feedback network. Thus, $V_{in(MPPC)}$ can be dynamically adjusted to enable the maximum power extraction from the HSMS282P based voltage doubler rectifier (see Fig. 2 (a)). If the applied nMOSFET is ultra-sensitive, the drain-to-source channel can be threshold with a current of several μA under ultra-small V_{GS} bias. Then equivalent $R_{DS,en}$ is achieved with a super I_3 current adjusting capability for the adaptive compensation loop control. When input power increases, the output current I_1 of the RF-DC rectifier rises as well as V_{in} in Fig. 3. Therefore, the implemented nMOSFET achieves more V_{GS} from the input voltage of LTC3129-1 with more $I_{D,max}$ to enable higher I_3. Then higher $V_{in(MPPC)}$ can be achieved in (2) since R_{high} is fixed, by which the adaptive compensation control is realized.

III. CIRCUIT DESIGN

In order to implement the internal reference V_{ref} for the adaptive compensation control design, nMOSFET drain connects the MPPC pin of the applied DC-DC converter to enable a constant V_{DS}=1.175V under maximum power transfer condition. While V_{GS} is biased through a high resistor voltage divider consisting of R_a and R_b to achieve an ultra-small $V_{GS}=V_{in}R_b/(R_a+R_b)$.

As $V_{in(MPPC)}$ increases with the incident power in

Table 1, the implemented high resistor voltage divider captures $V_{in(MPPC)}$ variation within incident powers from 21dBm to 24dBm. Then the captured $V_{GS}=V_{in}\cdot R_b/(R_a+R_b)$ biases the nMOSFET gate to enable current I_3 adjustment of the drain-to-source channel. Therefore, the equivalent current command $R_{DS,en}$ is realized, which compensates the $V_{in(MPPC)}$ in (2) dynamically for the maximum power extraction from a non-ideal source (e.g., a rectifier in Fig. 2 (a) once the incident RF power changes.

Accordingly, it demands the adopted nMOSFET with a high current sensitivity with small V_{GS} bias to threshold the drain-to-source current channel. Thus, an enhanced nMOSFET Si2342DS [7] is implemented to realize V_{GS} controlled $R_{DS,en}$ in (7). Meanwhile, V_{GS} should be ultra-small to ensure $R_{DS,en}$ ultra-high to minimize the current flowing through the drain-source channel of Si2342DS with V_{DS}=1.175V, due to which the voltage divider of R_a and R_b is high enough for current I_3 in (2) control requirement to capture different $V_{in(MPPC)}$ (see Table 1) simultaneously with a subtle power consumption. For accurate DC-IV measurement of the Si2342DS, an SMA based 24mil FR4 test fixture is fabricated in Fig. 4 (a). V_{GS} is swept from 0.4V to 0.58V with a high resistor voltage divider of R_a=620KΩ and R_b=51KΩ to sense and capture $V_{in(MPPC)}$ variation from 5.27V to7.61V exactly according to $V_{GS}=V_{in}R_b/(R_a+R_b)$ and maintains $V_{DS}=V_{ref}$ of the implemented DC-DC converter. The compensated ratio of R_{low}/R_{high} can be plotted with R_{low}=27KΩ and R_{high}=100KΩ, which is shown by the blue dotted curve (i.e., *Ratio-Compensate*) in Fig. 4 (b). By contrast, a fixed ratio of R_{low}/R_{high}=0.24 is provided with R_{low}=24 KΩ and R_{high}=100KΩ by a black dash curve (i.e., *Ratio-Fixed*) and optimal ratio of R_{low}/R_{high} is calculated with various $V_{in(MPPC)}$ from 5.27V to 7.61V in Table 1, which is plotted by a solid red curve (i.e., *Ratio-Optimal*).

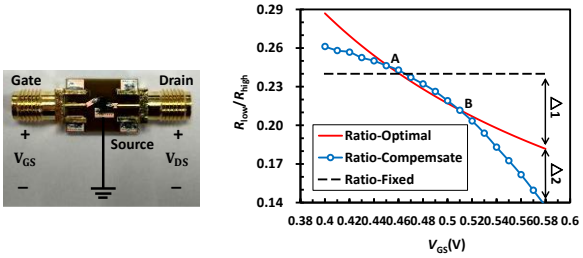

(a) (b)

Fig. 4. (a) SMA based DC-IV 24mil FR4 test fixture; (b) measurement of *Ratio-Compensate* with blue curve.

In this research, different V_{GS} would adaptively adjust the current I_3 in Fig. 5 based on $V_{in(MPPC)}$ from 5.27V to 7.61V in Table 1. The current I_3 with different V_{GS} can be precisely measured by the test fixture in Fig. 4 (a). Therefore, $V_{in(MPPC)}$ in (2) can be calculated with a fixed R_{high}=100KΩ. Then the ratio of R_{low}/R_{high} in (1) is achieved, which can be plotted as *Ratio-Compensate* curve in Fig. 4 (b) under different V_{GS}. For the comparison with the *Ratio-Compensate* curve, $V_{in(MPPC)}$ from 5.27V to 7.61V is normalized by $(R_a+R_b)/R_b$ (i.e., $V_{GS}=V_{in(MPPC)}R_b/(R_a+R_b)$) in the *Ratio-Optimal*. Then *Ratio_Optimal* can be achieved from R_{low}/R_{high} in Table 1 under different $V_{GS}=V_{in(MPPC)}R_b/(R_a+R_b)$. Thus, *Ratio-Compensate* and *Ratio-Optimal* can be plotted with same horizontal coordinate in Fig. 4 (b). There are two intersection points A and B between the *Ratio-Optimal* and *Ratio-Compensate* curves. When V_{GS} < 0.46V (i.e., $V_{in(MPPC)}$ =6.05V) satisfies at A, *Ratio-Compensate* curve is closer to *Ratio-Optimal* than *Ratio-Fixed*. Especially between A and B, *Ratio-Compensate* and *Ratio-Optimal* are almost unanimously. Whereas the *Ratio-Compensate* and *Ratio-Fixed* deviate in opposite direction compared to *Ratio-Optimal* when V_{GS} > 0.515V (i.e., $V_{in(MPPC)}$= 6.78V) at the intersection point B, delta ratio of the *Ratio-Fixed* and the *Ratio-Compensate* between *Ratio-Optimal* could be calculated with Δ_1=0.06 and Δ_2=0.04, which indicates the *Ratio-Compensate* precedes *Ratio-Fixed* even with a maximum input voltage V_{GS} = 0.58V (i.e., $V_{in(MPPC)}$=7.6V). Therefore, when V_{GS} increases from 0.4V to 0.58V (i.e., $V_{in(MPPC)}$ from 5.27V to7.61V in Table 1), the proposed adaptive compensation loop satisfies variation requirement of R_{low}/R_{high} for the overall $V_{in(MPPC)}$ in Table 1 within all power ranges of the implemented LTC3129-1 to maximize DC power transfer from HSMS282P based voltage doubler rectifier.

However, in the circuit design, it suggests that the bulk-boost DC-DC converter LTC3129-1 should be restricted with a maximum input voltage up to 15V [4]. Though HSMS282P based voltage doubler rectifier has a limited maximum output voltage of 15V due to its breakdown voltage [5], the semiconductor fabrication variation or other factors may cause breakdown voltage V_{br} more than 15V slightly, which will make its maximum output voltage more than 15V to damage LTC3129-1 permanently. Therefore, a 15V Zener diode is adopted for protection as shown in Fig. 5.

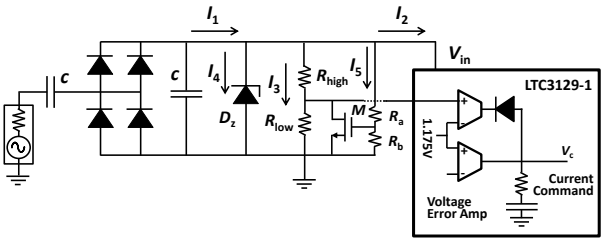

Fig. 5. Final proposed circuit with nMOSFET Si2342DS and 15V Zener diode (D_z).

The power conversion efficiency is more concerned in a WEC system. Thus, the power consumption caused

by Zener diode is analyzed and proven to be ultra-low if the switching frequency of LTC3129-1 is high enough. When open circuit voltage of HSMS282P based voltage doubler rectifier is more than 15V, a limited 15V for protection could only be applied as input voltage of the DC-DC converter LTC3129-1. Then the high resistor feedback network captures the input voltage to dynamically increase I_2 until the input voltage less than 15V. Meanwhile, linkage current I_4 of the Zener diode decreases to zero when input voltage less than 15V. This procedure responds transiently as switching frequency at PWM mode of LTC3129-1 is ultra-high of 1.2MHz [4] with a subtle power consumption. Therefore, the final circuit with a Si2342DS based adaptive compensation loop is proposed for the DC-DC converter to extract the maximum power transfer from the RF-DC rectifier as shown in Fig. 5.

IV. MEASUREMENT AND RESULTS

Three WPT receiver circuits are fabricated with LDO SPX3819 [3] and DC-DC bulk LTC3129-1 with/without nMOSFET based adaptive compensation control loop respectively as shown in Fig. 6 (a). HSMS282P Schottky diodes and several 0603 packaging passive elements are soldering on the 24mil FR4. For the measurement setup, signal generator AV1441A outputs 200 KHz RF signal. Then the RF signal is amplified by a commercial power amplifier (PA) and pre-calibrated by the spectrum analyzer AV4037. A 100 Ω load resistor is employed as a representative of the MCU and sensor networks. As these three WPT receiver circuits are designed with a fixed output steady DC voltage of 3.3V to satisfy minimum 100mW load power supply requirement, thus the output voltages along R_L are measured as shown in Fig. 6 (c). When the input power approaches 22.5dBm, the WPT receiver with a fixed ratio R_{low}/R_{high}=0.24 satisfy 100mW load power supply requirement at input power 22.5dBm and outperforms one with LDO SPX3819 from 22.5dBm to 24.5dBm. By comparison, Si2342DS based adaptive compensation loop of LTC3129-1 can further extract maximum DC power transfer from HSMS282P based voltage doubler rectifier over lower input powers. Measurement indicates that the power supply of 100mW with a output voltage around 3.3V can be achieved by the adaptive compensation loop based WPT receiver at 21.5dBm, which realizes an extended dynamic power range with a lower limit of 21.5dBm (22.5dBm for the fixed external high resistor network and 25dBm for the LDO SPX3819 in our previous work [8]) to realize a minimum 100mW load DC power delivery for the IPT enabled WEC system.

V. CONCLUSION

In this paper, an adaptive compensation loop control method is presented for dynamic range wireless power transfer (WPT) based wireless endoscopic capsules (WEC) applications. Rather than a fixed external resistor feedback network utilized in the DC-DC converter LTC3129-1, an enhanced nMOSFET Si2342DS based adaptive compensation loop is introduced to facilitate the maximum power transfer of the HSMS282P based voltage doubler rectifier from 21dBm to 24dBm, which can cover overall operational incident powers of the WEC system. Measurement validates that the proposed adaptive compensation loop control method realizes an extended dynamic power range with a lower limit of 21.5dBm to realize a minimum 100mW load DC power delivery for the IPT enabled WEC system. The method presented in this paper can be applied to combine with numerical solution to enable fast simulation of maximum power transfer efficiency based on coils modeling, which brings a practicality for an efficient IPT enabled WEC system.

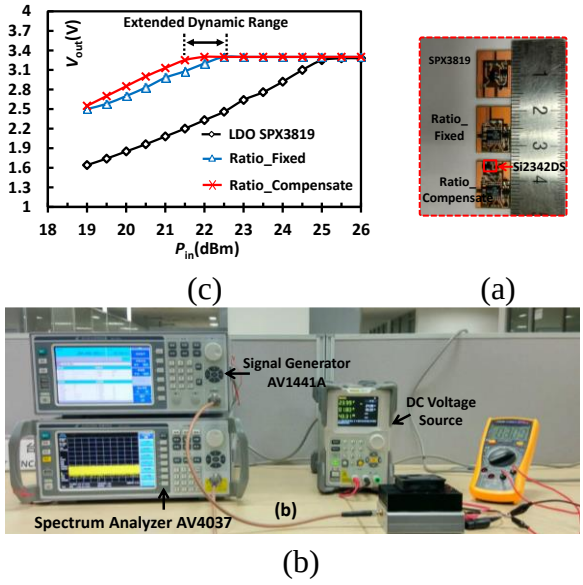

Fig. 6. (a) Fabrications of three applied WPT receivers; (b) measurement setup; (c) measurement results.

ACKNOWLEDGMENT

This work was supported in part by Singapore National Research Foundation Industry-IHL Partnership grant, in part by National Natural Science Foundation of China under the Grant No. 61401296, in part by the Natural Science Foundation for Youths of Jiangsu Province, China under Grant No. BK20130375 and Suzhou Science and Technology Council, China under Grant SYG201618.

REFERENCES

[1] G. Tortora, F. Mulana, G. Ciuti, P. Dario, and A. Menciassi, "Inductive-based wireless power recharging system for an innovative endoscopic capsule," *Energies*, vol. 8, no. 9, pp. 10315-10334,

2015.
[2] J. Zhiwei, Y. Guozheng, W. Zhiwu, and L. Hua, "Efficiency optimization of wireless power transmission systems for active capsule endoscopes," *Physiol. Meas.*, vol. 32, no. 10, p. 1561, 2011.
[3] T. A. Circuit, "Spx 3819 Electrical Characteristics," no. 510, 2008.
[4] Linear Technology, "LTC3129: 15V, 200mA Synchronous Buck-Boost DC/DC Converter with 1.3µA Quiescent Current," pp. 1-30, 2013.
[5] T.-W. Yoo and K. Chang, "Theoretical and experimental development of 10 and 35 GHz rectennas," *IEEE Trans. Microw. Theory Tech.*, vol. 40, no. 6, pp. 1259-1266, 1992.
[6] E. Falkenstein, M. Roberg, and Z. Popovic, "Low-power wireless power delivery," *IEEE Trans. Microw. Theory Tech.*, vol. 60, no. 7, pp. 2277-2286, 2012.
[7] Datasheet of Si2342DS: N-Channel 8V (D-S) MOSFET, Vishay Siliconix.
[8] H. Zhang, Z. Zhong, and W. Wu, "Extracting maximum efficiency of wireless power transfer in endoscopic capsule applications," in *Applied Computational Electromagnetics Society Symposium (ACES), 2017 International*, pp. 1-2, 2017.

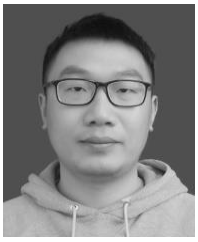

Hao Zhang was born in Jiangsu, China, in 1990. He received the B.Eng. degree from the School of Electronic and Optical Engineering, Nanjing University of Science and Technology, Nanjing, China, in 2014, where he is currently pursuing his Ph.D. degree. He was a Visiting Scholar with the Department of Electrical and Computer Engineering, National University of Singapore from July 2016 to July 2017. His current research interests include RF energy harvesting and wireless power transfer for biomedical applications and Internet of Things (IoTs).

Zheng Zhong received the B.Eng. and M.E. degrees from the University of Science and Technology of China, Hefei, China, in 2003 and 2006, respectively, and the Ph.D. degree in Microwave Engineering from the National University of Singapore (NUS), Singapore, in 2010. He has been a Research Fellow with the Department of Electrical and Computer Engineering, NUS, since 2010. His current research interests include RF/microwave semiconductor devices modeling and characterization, microwave and millimeterwave microwave integrated circuit/MMIC circuits design, and RF energy harvesting.

Wen Wu received the Ph.D. degree in Electromagnetic Field and Microwave Technology from Southeast University, Nanjing, China, in 1997. He is currently a Professor with the School of Electronic Engineering and Optoelectronic Technology, and an Associate Director of the Ministerial Key Laboratory of JGMT with the Nanjing University of Science and Technology, Nanjing, China. He has authored or co-authored over 240 journal and conference papers. He holds 14 patents. His current research interests include microwave and millimeter-wave theories and technologies, microwave and millimeter-wave detection, and multimode compound detection. Mr. Wu was the recipient of the Ministerial and Provincial-Level Science and Technology Awards six times.